



Interpretation of a multicomponent walkaway vertical seismic profile experiment

Bona Wu, Don C. Lawton, and Kevin W. Hall
CREWES, University of Calgary

Summary

A multicomponent walkaway VSP data was processed to study the rock properties of the target reservoir. Inversion and AVO attributes analysis showed no obvious gas effects in the studied interval. The observations were validated by production data. Post-stack PP-PS joint inversion was completed and compared to only P-wave inversion. Overall, they showed good consistency and the joint inversion added value to lithology prediction and fluid identification. This case study demonstrated that multicomponent VSP is an effective tool to predict rock properties, characterize the reservoir and monitor production.

Introduction

Due to its geometry, a VSP survey usually yields better resolution and a higher signal-to-noise ratio than surface seismic data. In addition, walkaway VSP geometry is suitable for AVO analysis. In this work, different rock properties were inverted from the VSP PP and PS image and prestack gathers. Interpretation of inversion and AVO attributes enabled us to better characterize the target reservoir and gave promise about how to integrate multicomponent VSP data into reservoir predicting and production monitoring.

The formation studied is a heavy oil reservoir in Canada. It was deposited as prograding tide-dominated deltas and composed of three stacked incised valleys. These incised valleys lie encased within regional deltaic, shoreface sands and marine muds. The depth of reservoir is about 500 m and it is made up of relatively unconsolidated shale-sand sequences, where fluid compressibility can have significant effect on the whole rock compressibility, which is then reflected on seismic data. Total thickness of the formation is approximately 50-75 meters (Hein et al., 2007) and it is an important resource of 9-10 API bitumen. The field is actively produced by steam assistant gravity drainage (SAGD).

The typical well logs in this area and from a nearby well are shown in Figure 1. In the reservoir zone, the gamma ray values are low which indicates clean sand deposits. High resistivity and porosity in these zones also indicate a good hydrocarbon reservoir. At the base of sand-filled valley, the resistivity becomes lower, which indicates bottom water. Above the bottom water zone is the transition zone.

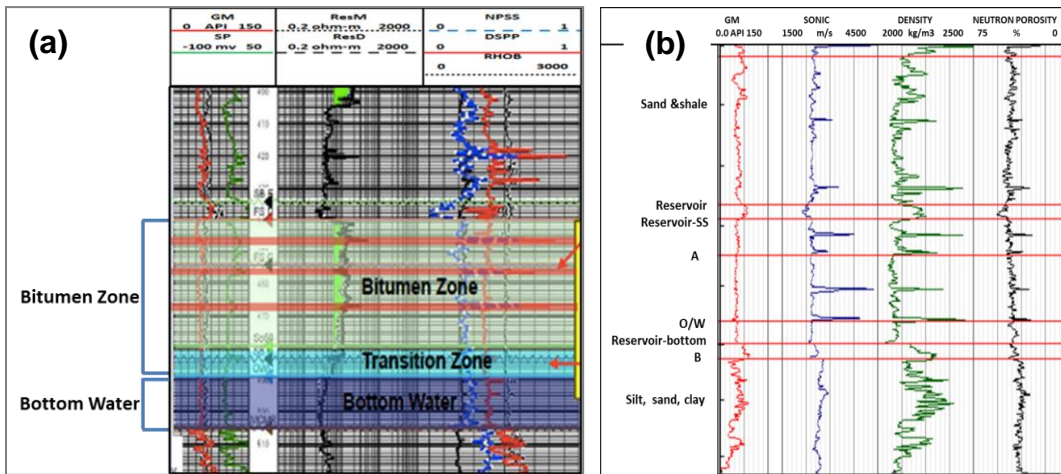


FIG. 1. (a) Typical logs of reservoir (from AER report) and (b) logs from well.

Inversion and AVO attributes analysis on P-wave data

Inversion and AVO attributes analysis helped to identify lithology and fluid changes inside the reservoir. An S-impedance vs P-impedance cross-plot is shown in Figure 2(a), which shows that the reservoir base has higher Z_s/Z_p . The cross-plot canceled out the effect of density (assuming that density has negligible changes). Therefore, it is the reciprocal of V_p/V_s which is higher at top of reservoir and lower at bottom of reservoir and they both follow an approximately linear trend.

V_p/V_s is also a good indicator of the sand and shale distribution. Based on the Greenberg and Castagna (1992) definition of different for commonly occurring lithologies, sand has slightly higher V_p/V_s than shale. Lower values of V_p/V_s which usually indicates saturation of hydrocarbon or water. If gas is present, the V_p/V_s is even lower than that for wet sands. Figure 2(b) shows a V_p/V_s vs P-wave impedance crossplot. Most of samples from the reservoir top (shale-sand contact, yellow and orange dots) are located in low impedance but high V_p/V_s zone while samples from the bottom of the reservoir (sand-shale contact, purple dots) are located in high P- impedance but low V_p/V_s zone. The crossplot also makes easier for us to identify the gas effects. If there is gas effect, it should locate at low P-wave impedance and low V_p/V_s zone (left bottom corner, marked by blue circle). Apparently, in our project reservoir, there are no gas effects.

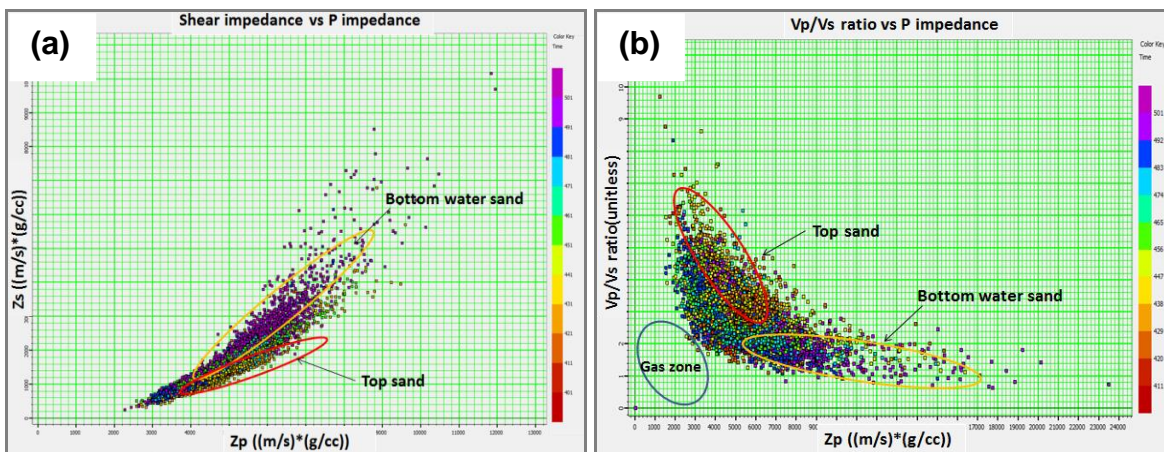


FIG. 2. (a) S-wave impedance vs P-wave impedance crossplot; (b) V_p/V_s vs P-wave impedance crossplot.

The top and bottom of the reservoir were identified by a cross-plot of inverted attributes. Lambda-Rho (LR) and Mu-Rho (MR) is another approach that helps to identify more details inside the reservoir. Mu-Rho (MR) vs Lambda-Rho (LR) cross-plot is shown in Figure 3. A $\lambda\rho$ vs $\mu\rho$ crossplot may minimize the effects of density and help to interpret the λ and μ attributes: The samples highlighted by yellow rectangle have negative $\lambda\rho$ values, probably caused by noise. The red rectangle zone should be a potential gas zone with low λ but high μ . Since there are only few samples in this interval, it evidenced that there are no gas effects in the reservoir. This result is consistent with the production data. The convincing cluster patterns can be seen in this cross-plot. For example, the samples from the overlying shale are highlighted by the grey circle with low compressibility and low rigidity; samples from the reservoir top (sand) are highlighted by red ellipse with slightly higher incompressibility and rigidity; samples from the reservoir sand are highlighted by blue ellipse which show very low incompressibility and rigidity; samples from the bottom water sand are highlighted by yellow circle which show similar incompressibility as the top reservoir sand but slightly higher rigidity. LMR is an effective tool to predict lithology and fluid in the studied reservoir.

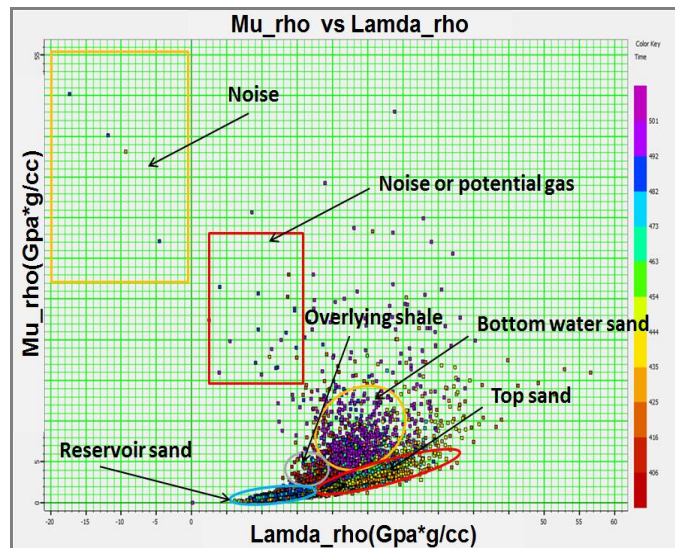


FIG. 3. Mu-rho vs Lambda_rho crossplot. The LMR crossplot helped to identify different lithologies and fluid changes of the reservoir.

PP- PS joint inversion

In this work, we also recorded and processed converted-wave data. Figure 4 shows post-stack PP-PS image registration. PS data has been transformed to PP time by picking the corresponding horizons on both datasets. Reservoir zone is highlighted by a yellow rectangle.

Joint PP-PS inversion can provide additional value and reduce risk or uncertainty in fluid/lithology discrimination and reservoir characterization. Figure 5 shows comparisons of S-impedance vs P-impedance cross-plots created from PP-PS joint version (a) and P-wave inversion (b). A cross-plot from PP-PS joint inversion shows the samples from the entire reservoir locate in four major zones. We can easily identify overlying shale, reservoir top sand, reservoir sand and bottom water sand on the cross-plot while this distribution doesn't show on P-wave inversion cross-plot. The comparison validated that the information from S-wave data improved accuracy of prediction of lithology and fluid in the reservoir zone.

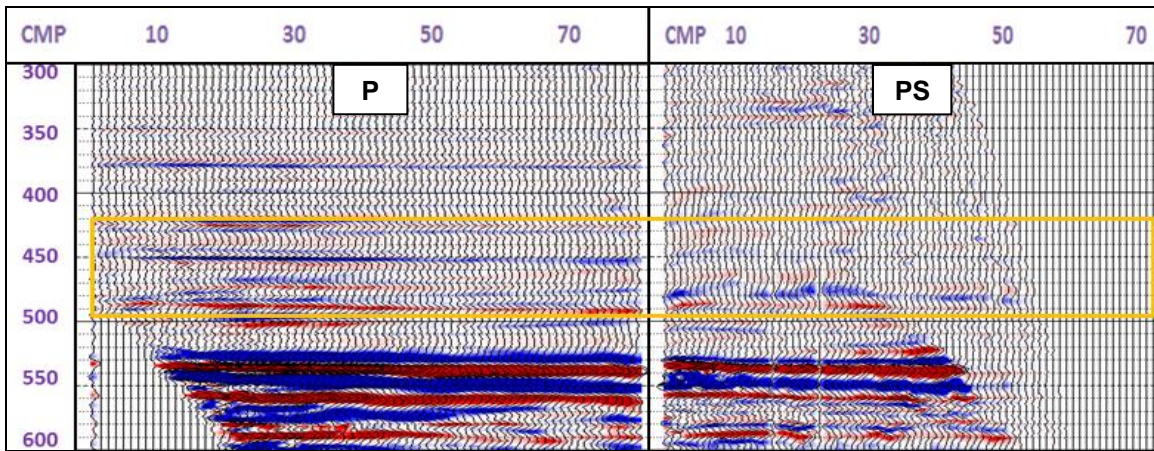


FIG.4. Registration of PP and PS data. Reservoir zone is highlighted by a yellow rectangle.

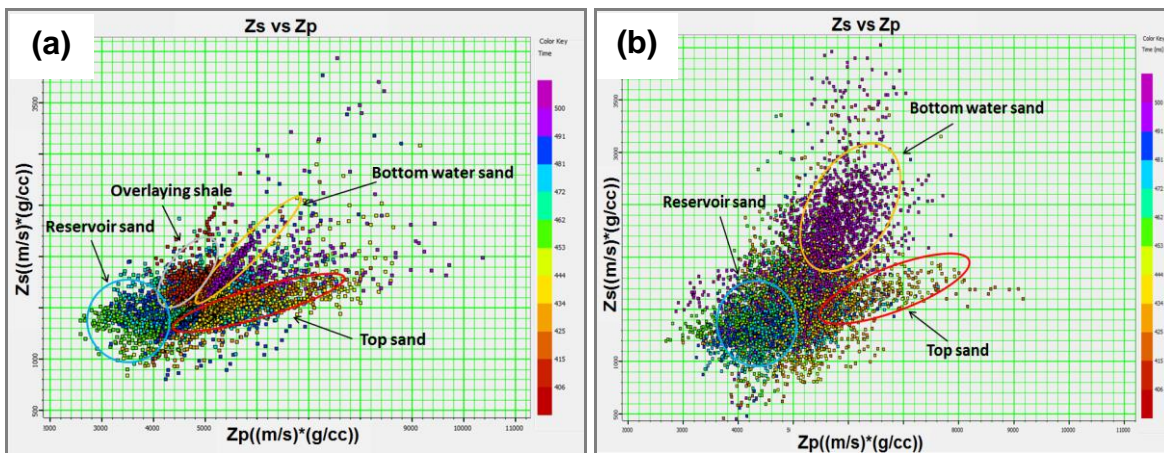


FIG. 5. Comparison of PP-PS joint inversion and P-wave only inversion. (a) Crossplot of S-impedance vs P-impedance inverted from PP-PS joint inversion; (b) crossplot of S-impedance vs P-impedance inverted from P-wave inversion.

Conclusions

Due to the advantage of VSP geometry, the hydrocarbon effects may be more visible on VSP data than surface seismic sections. In this work, we successfully applied VSP data analysis to predict rock properties and monitor production. Properties analysis showed no obvious gas effects in the studied interval which was validated by production data. PP-PS joint inversion added value to P-wave only interpretation. Inverted rock properties and their cross-plots, AVO Lambda-mu-rho analysis are effective tools to predict lithologies and hydrocarbon in the target reservoir. However, the lower resolution of the PS image and the distance of the well and VSP borehole as well as the absence of S-wave log may degrade the reliability of the detailed interpretation.

Acknowledgements

We thank an anonymous company for providing the VSP data for this research and for permission to publish the results. We thank GEDCO/Schlumberger for providing the VISTA software and technical support during the data processing. We also thank CGG/Hampson-Russell for their inversion and AVO software. Finally, we give thanks to all of the CREWES sponsors for support of this research. We also gratefully acknowledge support from NSERC (Natural Science and Engineering Research Council of Canada) through the grant CRDPJ 379744-08.

References

- Bubshait, S., 2010, VSP processing for coal reflections: M.Sc. Thesis, University of Calgary.
- Castagna, J. P., Batzle, M. L., and Eastwood, R. L., 1985, Relationships between compressional-wave and shear-wave velocities in clastic silicate rocks: *Geophysics* 50, 571–581.
- Castagna, J. P., Swan, H. W., and Foster, D. J., 1998, Framework for AVO gradient and intercept interpretation: *Geophysics*, 63, 948–956.
- Chopra, S., Alexeev, V., Xu, Y., 2003, Successful AVO and Cross-plotting: *Canada CSEG recorder*, 28 No. 09.
- Coulombe, C.A., Stewart, R.R., and Jones, M.J., 1996, AVO processing and interpretation of VSP data: *Canadian Journal of Exploration Geophysics*, 32, 41-62.
- Greenberg, M. L. and Castagna, J. P., 1992, Shear-wave velocity estimation in porous rocks: theoretical formulation, preliminary verification and applications: *Geophysical Prospecting*, 40, 195-209
- Hall, K. W., Lawton, D. C., Holloway, D., and Gallant, E.V., 2012, Walkaway 3C-VSP, CREWES Research Report, Volume 24.
- Hein, F., Weiss, J., and Berhane, H., 2007, Cold Lake Oil Sands Area: Formation Picks and Correlation of Associated Stratigraphy: The Alberta Energy and Utilities Board/ Alberta Geological Survey (EUB/AGS) Geo-Note, 2006-03.
- Hinds, R.C., Anderson, N.L., and Kuzmiski, R.D., 2007, VSP interpretative processing: Theory and practice, SEG Continuing Education Course Notes.
- Hinds, R.C., and Kuzmiski, R.D., 2001, VSP for the interpreter/processor for 2001 and beyond: part1, *CSEG Recorder*, 26, No.9, 84-95.
- Lawton, D.C, Gary, M. F., and Stewart, R. R., 2012, Reflections on PS: An interactive discussion of problems and promise in converted-wave exploration: *CREWES Research Report*, 24, 58.
- Lines, L.R., and Newrick, R.T., 2004, Fundamentals of geophysical interpretation, *Geophysical Monograph Series: Society of Exploration Geophysicists*.
- Shuey, R. T., 1985, A simplification of the Zoeppritz equations: *Geophysics* 50, 609–614.
- Wu, B., Lawton, D.C, and Hall, K., 2014, Analysis of multicomponent walkaway vertical seismic profile data: *CREWES Research Report*, 26, 79.
- Zhang, John J. and Bentley, Laurence R., 2005, Factors determining Poisson's ratio, *CREWES Research Report*, 17, 62.